DETERMINATION OF V_{cb} AND V_{ub}

Written October 2005 by R. Kowalewski (Univ. of Victoria, Canada) and T. Mannel (Univ. of Siegen, Germany)

INTRODUCTION

Precision determinations of $|V_{ub}|$ and $|V_{cb}|$ are central to testing the CKM sector of the Standard Model, and complement the measurements of CP asymmetries in B decays. The length of the side of the unitarity triangle opposite the well-measured angle β is proportional to the ratio $|V_{ub}|/|V_{cb}|$, making its determination a high priority of the heavy flavor physics program.

The quark transitions $b \to c\ell\overline{\nu}_\ell$ and $b \to u\ell\overline{\nu}_\ell$ provide two avenues for determining these CKM matrix elements, namely through inclusive and exclusive final states. The experimental and theoretical techniques underlying these two avenues are independent, providing a crucial cross-check on our understanding. Significant progress has been made in both approaches since the previous reviews of $|V_{cb}|$ [1] and $|V_{ub}|$ [2].

The theory underlying the determination of $|V_{qb}|$ is mature. The theoretical approaches all use the fact that the mass m_b of the b quark is large compared to the scale $\Lambda_{\rm QCD}$ that determines low-energy hadronic physics. The basis for precise calculations is a systematic expansion in powers of $\Lambda_{\rm QCD}/m_b$, where effective-field-theory methods are used to separate non-perturbative from perturbative contributions. The expansion in $\Lambda_{\rm QCD}/m_b$ and α_s works well enough to enable a precision determination of $|V_{cb}|$ and $|V_{ub}|$ in semileptonic decays.

The large data samples available at the B factories have opened up new possibilities experimentally. Analyses where one B meson from an $\Upsilon(4S)$ decay is fully reconstructed allow a recoiling semileptonic B decay to be studied with higher purity than was previously possible. Improved knowledge of $\overline{B} \to X_c\ell\overline{\nu}_\ell$ decays allows partial rates for $\overline{B} \to X_u\ell\overline{\nu}_\ell$ transitions to be measured in regions previously considered inaccessible, increasing the acceptance for $\overline{B} \to X_u\ell\overline{\nu}_\ell$ transitions and reducing theoretical uncertainties.

At present the inclusive determinations of both $|V_{cb}|$ and $|V_{ub}|$ are more precise than the corresponding exclusive determinations. Improvement of the exclusive determinations remains an important goal, and future progress, in particular in lattice QCD, may provide this.

Throughout this review the numerical results quoted are based on the methods of the Heavy Flavor Averaging Group [3].

DETERMINATION OF V_{cb}

Summary: The determination of $|V_{cb}|$ from exclusive decays is currently at a relative precision of about 4%. The main limitation is the knowledge of the form factor near the maximum momentum transfer to the leptons. Further progress from lattice calculations of the form factors is needed to improve the precision.

Determinations of $|V_{cb}|$ from inclusive decays are currently at a level of 2% relative uncertainty. The limitations arise mainly from our ignorance of higher order perturbative and non-perturbative corrections.

The values obtained from inclusive and exclusive determinations are consistent with each other:

$$|V_{cb}| = (41.5 \pm 0.7) \times 10^{-3} \text{ (inclusive)} \tag{1}$$

$$|V_{cb}| = (40.9 \pm 1.8) \times 10^{-3} \text{ (exclusive).} \tag{2}$$

While this consistency may be viewed as a validation, in which case further reduction of the uncertainty is unwarranted, we nevertheless provide an average value,

$$|V_{cb}| = (41.4 \pm 0.6) \times 10^{-3} \ . \tag{3}$$

$|V_{cb}|$ from exclusive decays

Exclusive determinations of $|V_{cb}|$ are based on a study of semileptonic B decays into the ground state charmed mesons D and D^*. The main uncertainties in this approach stem from our ignorance of the form factors describing the $B \to D$ and $B \to D^*$ transitions. However, in the limit of infinite bottom and charm quark masses only a single form factor appears, the

Isgur-Wise function [4], which depends on the product of the four-velocities v and v' of the initial and final-state hadrons.

The method used for the extraction of $|V_{cb}|$ refers to the spectrum in the variable $w \equiv v \cdot v'$ corresponding to the energy of the final state $D^{(*)}$ meson in the rest frame of the decay. Heavy Quark Symmetry (HQS) [4,5] predicts the normalization of the rate at $w = 1$, the maximum momentum transfer to the leptons, and $|V_{cb}|$ is obtained from an extrapolation of the spectrum to $w = 1$.

A precise determination requires corrections to the HQS prediction for the normalization as well as some information on the slope of the form factors near the point $w = 1$, since the phase space vanishes there. The corrections to the HQS prediction due to finite quark masses is given in terms of the symmetry-breaking parameter

$$\frac{1}{\mu} = \frac{1}{m_c} - \frac{1}{m_b} ,$$

which is practically $1/m_c$ for realistic quark masses. HQS ensures that the matrix elements corresponding to the currents that generate the HQS are normalized at $w = 1$, which means that some of the form factors either vanish or are normalized at $w = 1$. Due to Luke's Theorem [6](which is an application of the Ademollo-Gatto theorem [7] to heavy quarks), the leading correction to those form factors normalized due to HQS is quadratic in $1/\mu$, while for the form factors that vanish in the infinite mass limit the corrections are in general linear in $1/m_c$ and $1/m_b$. Thus we have, using the definitions as in Eq. (2.84) of Ref. [8]

$$\begin{aligned} h_i(1) &= 1 + \mathcal{O}(1/\mu^2) \qquad \text{for} i = +, V, A_1, A_3 \ , \\ h_i(1) &= \mathcal{O}(1/m_c,\, 1/m_b) \qquad \text{for} i = -, A_2 \ . \end{aligned} \tag{4}$$

In addition to these corrections there are perturbatively calculable radiative corrections from QCD and QED, which will be discussed in the relevant sections. Both - radiative corrections as well as $1/m$ corrections - are considered in the

framework of Heavy Quark Effective Theory (HQET) [9], which provides for a systematic expansion.

$\overline{B} \to D^* \ell \overline{\nu}_\ell$

The decay rate for $\overline{B} \to D^* \ell \overline{\nu}_\ell$ is given by

$$\frac{d\Gamma}{dw}(\overline{B} \to D^* \ell \overline{\nu}_\ell) = \frac{G_F^2}{48\pi^3}|V_{cb}|^2 m_{D^*}^3 (w^2-1)^{1/2} P(w)(\mathcal{F}(w))^2 \tag{5}$$

where $P(w)$ is a phase space factor with $P(1) = 12(m_B - m_{D^*})^2$ and $\mathcal{F}(w)$ is dominated by the axial vector form factor h_{A_1} as $w \to 1$. In the infinite-mass limit, the HQS normalization gives $\mathcal{F}(1) = 1$.

The form factor $\mathcal{F}(w)$ is parametrized as

$$\mathcal{F}(w) = \eta_{\rm QED}\eta_{\rm A}\left[1 + \delta_{1/m^2} + \cdots\right] + (w-1)\rho^2 + \mathcal{O}((w-1)^2) \tag{6}$$

where the QED [10] and QCD [11] short distance radiative corrections are

$$\eta_{\rm QED} = 1.007\,, \quad \eta_{\rm A} = 0.960 \pm 0.007 \tag{7}$$

and δ_{1/m^2} comes from non-perturbative $1/m^2$ corrections. Analyticity and unitarity may be used to restrict the form factors [12,13] from which the bound $-0.17 < \rho^2 < 1.51$ is obtained.

Recently, lattice simulations with finite quark masses have become possible, and have been used to calculate the deviation of $\mathcal{F}(1)$ from unity. The value quoted from these calculations, which still use the "quenched" approximation, is [14]

$$\mathcal{F}(1) = 0.919^{+0.030}_{-0.035} \tag{8}$$

where the errors quoted in Ref. [14] have been added in quadrature and the QED correction has been taken into account. This value is compatible with estimates based on non-lattice methods.

Many experiments [15–21] have measured the differential rate as a function of w. Fig. 1 shows the measured values and corresponding average of the product $|V_{cb}|F(1)$ and the slope ρ^2. The confidence level of the average is $\sim 1\%$, suggesting the need for further experimental work. The leading sources of

experimental uncertainty come from the uncertainties on the form factor ratios $R_1 \propto A_2/A_1$ and $R_2 \propto V/A_1$, and on the background due to $\overline{B} \to D^* \pi \ell \overline{\nu}_\ell$ decays, along with particle reconstruction efficiencies. These can be significantly reduced with B-factory data sets. Using the value given above for $\mathcal{F}(1)$ and the average $|V_{cb}|\mathcal{F}(1)$=(37.6±0.9) $\times 10^{-3}$ gives

$$|V_{cb}| = (40.9 \pm 1.0_{\rm exp}{}^{+1.6}_{-1.3}{}_{\rm theo}) \times 10^{-3}. \tag{9}$$

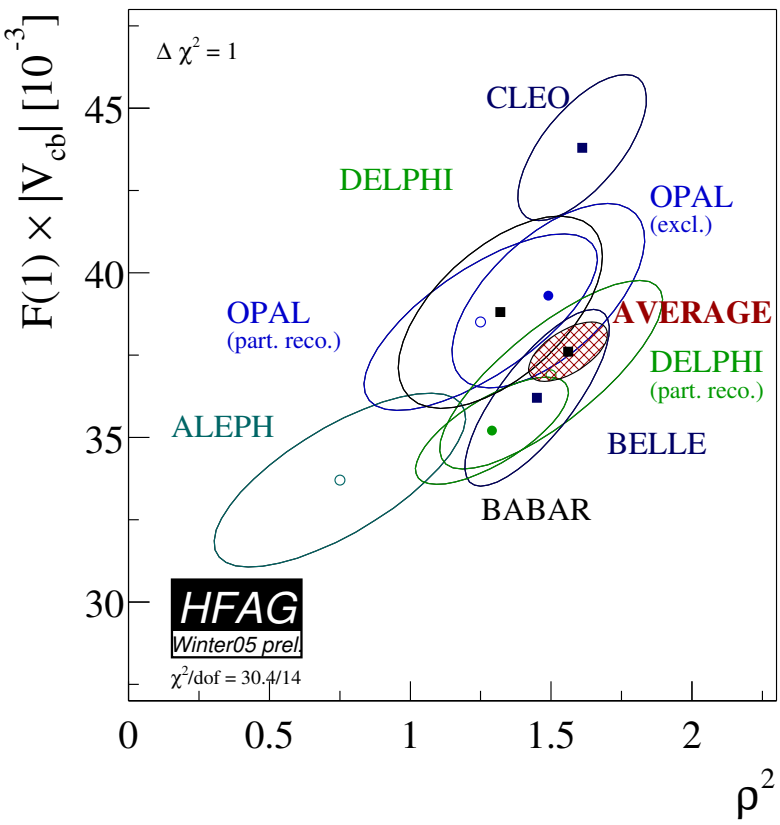

Figure 1: Measurements of $|V_{cb}|\mathcal{F}(1)$ and ρ^2 along with the average determined from a χ^2 fit. The hatched area corresponds to the $\Delta\chi^2 = 1$ contour. This plot is taken from [3].

$\overline{B} \to D\ell\overline{\nu}_\ell$

The differential rate for $\overline{B} \to D\ell\overline{\nu}_\ell$ is given by

$$\frac{d\Gamma}{dw}(\overline{B} \to D\ell\overline{\nu}_\ell) = \frac{G_F^2}{48\pi^3}|V_{cb}|^2(m_B + m_D)^2 m_D^3 (w^2-1)^{3/2}(\mathcal{G}(w))^2. \tag{10}$$

The form factor is

$$\mathcal{G}(w) = h_+(w) - \frac{m_B - m_D}{m_B + m_D} h_-(w), \tag{11}$$

where h_+ is normalized due to HQS and h_- vanishes in the heavy mass limit. Thus

$$\mathcal{G}(1) = 1 + \mathcal{O}\left(\frac{m_B - m_D}{m_B + m_D}\frac{1}{m_c}\right) \tag{12}$$

and the corrections to the HQET predictions are parametrically larger than was the case for $\overline{B} \to D^*\ell\overline{\nu}_\ell$.

However, it has been argued recently that the limit in which the kinetic energy μ_π^2 is equal to the chromomagnetic moment μ_G^2 (these quantities are discussed below in more detail) may be useful, and that deviations from this limit could be treated as small perturbations [22]. For the form factors this limit has quite far-reaching consequences, in particular it implies that for the $B \to D$ form factor the relations valid in the heavy mass limit hold in all orders in the $1/m_Q$ expansion. Based on these arguments

$$\mathcal{G}(1) = 1.04 \pm 0.01_{\rm power} \pm 0.01_{\rm pert} \tag{13}$$

is derived in Ref. [22]. If this notion gains acceptance, it could provide a rationale for reducing the uncertainties in $\mathcal{G}(1)$ from undetermined contributions of order $1/m_Q^4$.

Recently, lattice calculations that do not refer to the heavy mass limit have become available, and hence the fact that deviations from the HQET predictions are parametrically larger than in the case $\overline{B} \to D^*\ell\overline{\nu}_\ell$ is irrelevant. These calcuations quote a (preliminary) value [23]

$$\mathcal{G}(1) = 1.074 \pm 0.018 \pm 0.016 \tag{14}$$

which has an error comparable to the one quoted for $\mathcal{F}(1)$, although some uncertainties have not been taken into accounted.

The existing measurements of $|V_{cb}|\mathcal{G}(1)$ and ρ^2 are shown in Fig. 2, resulting in an average value $|V_{cb}|\mathcal{G}(1) = (42.2 \pm 3.7) \times 10^{-3}$. Using the value given above for $\mathcal{G}(1)$, accounting for the QED correction and conservatively adding the theory uncertainties linearly results in

$$|V_{cb}| = (39.0 \pm 3.4 \pm 3.0) \times 10^{-3} \tag{15}$$

where the first uncertainty is from experiment and the second from theory.

Measuring the differential rate at $w = 1$ is more difficult in $\overline{B} \to D\ell\overline{\nu}_\ell$ decays than in $\overline{B} \to D^*\ell\overline{\nu}_\ell$ decays, since the rate is smaller and the background from mis-reconstructed $\overline{B} \to D^*\ell\overline{\nu}_\ell$ decays is significant; this is reflected in the larger experimental uncertainty. The B factories may be able to address these limitations by studying decays recoiling against fully reconstructed B mesons or doing a global fit to $\overline{B} \to X_c\ell\overline{\nu}_\ell$ decays. Prospects for precise measurements of the total $\overline{B} \to D\ell\overline{\nu}_\ell$ rate are better, so theoretical input on the shape of the w spectrum in $\overline{B} \to D\ell\overline{\nu}_\ell$ is valuable.

Prospects for Lattice determinations of the $B \to D^{(*)}$ form factors

The prospects for lattice determinations of the $B \to D^{(*)}$ form factors in the near term are rosy, because calculations with realistic sea quarks have begun to appear. The key [14,24] is a set of double-ratios, constructed so that all uncertainties scale with the deviation of the form factor from unity.

One of the important uncertainties in the existing lattice calculations is the chiral extrapolation, namely, the extrapolation from the light quark masses used in the numerical lattice computation to the up and down quark masses. This is under very good control for the $B \to D$ transition, but for $B \to D^*$ is complicated by the coincidence $m_\pi \approx m_{D^*} - m_D$. As a consequence, one must have exceptional analytic control over the

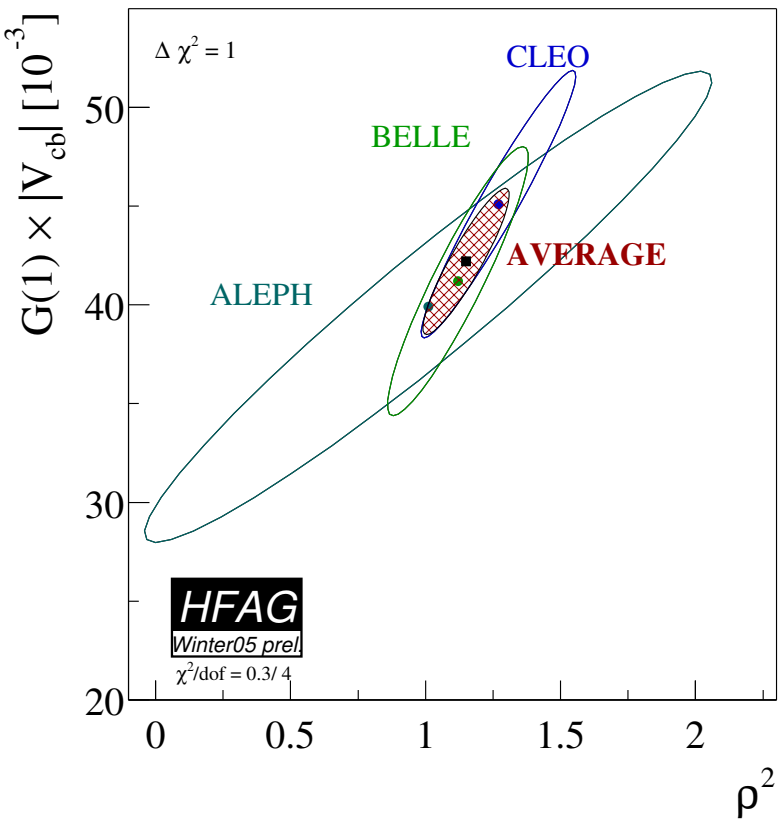

Figure 2: Measurements of $|V_{cb}|\mathcal{F}(1)$ and ρ^2 along with the average determined from a χ^2 fit. The hatched area corresponds to the $\Delta\chi^2 = 1$ contour. This plot is taken from [3].

extrapolation, including modifications of chiral perturbation theory for lattice QCD with non-zero lattice spacing.

With these developments, it will be possible to obtain full-QCD values for $\mathcal{F}(1)$ and $\mathcal{G}(1)$. The projected uncertainty will be 2-3%. This is not much smaller than before, but the foundation will be more reliable. This uncertainty needs to improve further to be comparable to the projected 1% uncertainty for the inclusive determination of $|V_{cb}|$.

To reach the target of 1% theoretical uncertainty more analytical work is needed. In lattice QCD, heavy-quark discretization effects are controlled by using HQET to match lattice gauge theory to continuum QCD, order-by-order in the

heavy-quark expansion [25–28]. This matching must be carried out to higher order, and some of this is in progress [29,30]. But some aspects, such as the radiative corrections to the $1/m_Q$ corrections to the transition currents, and the $1/m_Q^2$ corrections to the currents, are not yet underway. The task involved is comparable to, perhaps a bit greater than, the effort needed for carrying out the heavy-quark expansion for the inclusive method to the same order.

$|V_{cb}|$ from inclusive decays

At present the most precise determinations of $|V_{cb}|$ come from inclusive decays. The method is based on a measurement of the total semileptonic decay rate, together with the leptonic energy and the hadronic invariant mass spectra of inclusive semileptonic decays. The total decay rate can be calculated quite reliably in terms of non-perturbative parameters that can be extracted from the information contained in the spectra.

Inclusive semileptonic rate

The theoretical foundation for the calculation of the total semileptonic rate is the Operator Product Expansion (OPE) which yields the Heavy Quark Expansion (HQE), a systematic expansion in inverse powers of the b-quark mass [31,32]. The validity of the OPE is proven in the deep euclidean region for the momenta (which is satisfied, *e.g.*, in deep inelastic scattering), but its application to heavy quark decays requires a continuation to time-like momenta $p_B^2 = M_B^2$, where possible contributions which are exponentially damped in the euclidean region could become oscillatory. The validity of the OPE for inclusive decays is equivalent to the assumption of parton-hadron duality, hereafter referred to simply as duality, and possible oscillatory contributions would be an indication of duality violation.

Duality-violating effects are in fact hard to quantify; in practice they would appear as unnaturally large coefficents of higher order terms in the $1/m$ expansion [33]. Present fits include terms up to order $1/m_b^3$, the coefficients of which have sizes as expected a priori by theory. The consistency of the data with these OPE fits will be discussed later; no indication is

found that terms of order $1/m_b^4$ or higher are large, and there is no evidence for duality violations in the data. Thus duality or, likewise, the validity of the OPE, is assumed in the analysis, and no further uncertainty is assigned to possible duality violations.

The OPE result for the total rate can be written schematically (the details of the expression can be found, *e.g.*, in [34]) as

$$\Gamma = |V_{cb}|^2 \hat{\Gamma}_0 m_b^5(\mu)(1 + A_{ew}) A^{\rm pert}(r,\mu) \times \left[z_0(r) + z_2(r) \left(\frac{\mu_\pi^2}{m_b^2}, \frac{\mu_G^2}{m_b^2} \right) + z_3(r) \left(\frac{\rho_{\rm D}^3}{m_b^3}, \frac{\rho_{\rm LS}^3}{m_b^3} \right) + ... \right] \quad (16)$$

where A_{ew} denotes the electroweak and $A^{\rm pert}(r,\mu)$ the QCD radiative corrections, r is the ratio m_c/m_b and the z_i are known phase-space functions. The expression is known up to $1/m_b^3$, where the HQE parameters are given in terms of forward matrix elements by

$$\begin{aligned} \overline{\Lambda} &= M_B - m_b \\ \mu_\pi^2 &= -\langle B|\overline{b}(iD_\perp)^2 b|B\rangle \\ \mu_G^2 &= \langle B|\overline{b}(iD_\perp^\mu)(iD_\perp^\nu)\sigma_{\mu\nu} b|B\rangle \\ \rho_{\rm D}^3 &= \langle B|\overline{b}(iD_{\perp\mu})(ivD)(iD_\perp^\nu) b|B\rangle \\ \rho_{\rm LS}^3 &= \langle B|\overline{b}(iD_\perp^\mu)(ivD)(iD_\perp^\nu)\sigma_{\mu\nu} b|B\rangle \end{aligned} \quad (17)$$

The non-perturbative matrix elements depend on the renormalization scale μ, on the chosen renormalization scheme and on the quark mass m_b. The rates and the spectra depend strongly on m_b (or equivalently on $\overline{\Lambda}$), which makes the discussion of renormalization issues mandatory.

Using the pole mass definition for the heavy quark masses, it is well known that the corresponding perturbative series of decay rates does not converge very well, making a precision determination of $|V_{cb}|$ in such a scheme impossible. The solution to this problem is either to chose an appropriate "short-distance" mass definition, as in the kinetic scheme [35,36], or to eliminate the heavy quark mass in favor of a physical observable, such as the $\Upsilon(1S)$ mass (a well-defined short-distance mass up to

α_s^3), as in the 1S scheme [37]. Both of these schemes have been applied to semi-leptonic $b \to c$ transitions, yielding comparable results and uncertainties.

The 1S scheme eliminates the b quark pole mass by relating it to the mass of the 1S state of the Υ system. The ratio of these two masses can be computed perturbatively, assuming that possible non-perturbative contributions to the $\Upsilon(1S)$ mass are small. This is supported by an estimate performed in Ref. [38]. Eliminating the b quark pole mass in the semileptonic rate in favor of the $\Upsilon(1S)$ mass yields an expansion that converges rapidly.

Alternatively one may use a short-distance mass definition such as the $\overline{\rm MS}$ mass $m_b^{\overline{\rm MS}}(m_b)$. However, it has been argued that the scale m_b is unnaturally high for B decays, while for smaller scales $\mu \sim 1$ GeV $m_b^{\overline{\rm MS}}(\mu)$ is under poor control. For this reason the so-called "kinetic mass" $m_b^{\rm kin}(\mu)$, has been proposed. It is the mass entering the non-relativistic expression for the kinetic energy of a heavy quark, and is defined using heavy quark sum rules [36].

The HQE parameters also depend on the renormalization scale and scheme. The matrix elements displayed in Eq. (17) are defined with the full QCD fields and states, which is the definition employed in the kinetic scheme. In the 1S scheme, one usually uses the parameters λ_1 and λ_2 which are defined in the infinite mass limit. The relation between these parameters is

$$\begin{aligned} \overline{\Lambda}_{\rm HQET} &= \lim_{m_b\to\infty} \overline{\Lambda}\,, \quad -\lambda_1 = \lim_{m_b\to\infty} \mu_\pi^2 \\ \lambda_2 &= \lim_{m_b\to\infty} \mu_G^2\,, \quad \rho_1 = \lim_{m_b\to\infty} \rho_D^3 \\ \rho_2 &= \lim_{m_b\to\infty} \rho_{LS}^3 \end{aligned}$$

Defining the kinetic energy and the chromomagnetic moment in the infinite-mass limit (as, *e.g.*, in the 1S scheme) requires that $1/m_b$ corrections to the matrix elements defined in Eq. (17) be taken into account once one goes beyond order $1/m_b^2$. As a result, additional quantities $\mathcal{T}_1 \cdots \mathcal{T}_4$ appear at order $1/m_b^3$. However, these quantities are correlated such that

the total number of non-perturbative parameters to order $1/m_b^3$ is the same as in the scheme where m_b is kept finite in the matrix elements which define the non-perturbative parameters. A detailed discussion of these issues can be found in [39].

In order to define the HQE parameters properly one must adopt a renormalization scheme, as was done for the heavy quark mass. Since all these parameters can again be determined by heavy quark sum rules, one may adopt a scheme similar to the kinetic scheme for the quark mass. The HQE parameters in the kinetic scheme depend on powers of the renormalization scale μ, and the above relations are valid in the limit $\mu \to 0$, leaving only logarithms of μ.

Some of these parameters also appear in the relation for the heavy hadron masses. The quantity $\overline{\Lambda}$ is determined once a definition is specified for the quark mass. The parameter μ_G^2 can be extracted from the mass splitting in the lowest spin-symmetry doublet of heavy mesons

$$\mu_G^2(\mu) = \frac{3}{4} C_G(\mu, m_b)(M_{B^*}^2 - M_B^2) \tag{18}$$

where $C_G(\mu, m_b)$ is a perturbatively-computable coefficient which depends on the scheme. In the kinetic scheme we have

$$\mu_G^2(1\mathrm{GeV}) = 0.35^{+0.03}_{-0.02}\,\mathrm{GeV}^2. \tag{19}$$

To relate these to the HQET parameters one needs to perform a change of schemes. As a rule of thumb one has, up to order α_s,

$$\begin{aligned} \overline{\Lambda}_{\mathrm{HQET}} &= \overline{\Lambda}^{\mathrm{kin}}(1\mathrm{GeV}) - 0.255\,\mathrm{GeV} \\ -\lambda_1 &= \mu_\pi^2(1\mathrm{GeV}) - 0.18\,(\mathrm{GeV})^2\,. \end{aligned}$$

Determination of HQE Parameters and $|V_{cb}|$

Several experiments have measured moments in $\overline{B} \to X_c \ell \overline{\nu}_\ell$ decays [40–48] as a function of the minimum electron momentum. The measurements of the moments of the electron energy spectrum (0th-3rd) and of the squared hadronic mass spectrum (0th-2nd) have statistical uncertainties that are roughly equal to

their systematic uncertainties. They can be improved with more data and significant effort. Measurements of photon energy moments ($0^{\rm th}$-$2^{\rm nd}$) in $B \to X_s\gamma$ decays [49–52] as a function of the minimum accepted photon energy are still primarily statistics limited. Global fits to these moments [53–56] have been performed in the 1S and kinetic schemes. A global fit to a large set of hadron mass, electron energy and photon energy moments in the 1S scheme gives [55]

$$|V_{cb}| = (41.4 \pm 0.6 \pm 0.1) \times 10^{-3} \tag{20}$$

$$m_b^{\rm 1S} = 4.68 \pm 0.03\,{\rm GeV} \tag{21}$$

$$\lambda_1^{\rm 1S} = -0.27 \pm 0.04\,{\rm GeV} \tag{22}$$

where the first error includes experimental and theoretical uncertainties and the second error on $|V_{cb}|$ comes from the B lifetime. The same data along with some recent measurements of the $\overline{B} \to X_s\gamma$ energy moments have been fitted in the kinetic scheme, resulting in [56]

$$|V_{cb}| = (41.58 \pm 0.45 \pm 0.58) \times 10^{-3} \tag{23}$$

$$m_b^{\rm kin} = 4.591 \pm 0.040\,{\rm GeV} \tag{24}$$

$$\mu_\pi^2({\rm kin}) = 0.406 \pm 0.042\,{\rm GeV} \tag{25}$$

where the first error includes statistical and theoretical uncertainties and the second error on $|V_{cb}|$ is from the estimated accuracy of the HQE for the total semileptonic rate. The mass value may be compared with what is extracted from the threshold region of $e^+e^- \to b\overline{b}$ [57]:

$$m_b^{\rm kin} = 4.56 \pm 0.06\,{\rm GeV}. \tag{26}$$

In each case, theoretical uncertainties are estimated and included in performing the fits. Similar values for the parameters are obtained when only experimental uncertainties are used in the fits. The parameters determined from separate fits to electron energy moments and hadronic mass moments in semileptonic decays are compatible with each other and with

those obtained from moments of the $\overline{B} \to X_s\gamma$ photon energy spectrum. The fit quality is good; the χ^2/dof is 17.6/41 (50.9/86) for the fit in the kinetic (1S) scheme, suggesting that the theoretical uncertainties may be overestimated, and showing no evidence for duality violations at a significant level. That said, a reliable method for quantifying the uncertainties from duality remains elusive.

The fits in the two schemes agree well on $|V_{cb}|$. We take the arithmetic averages of the values and of the errors to quote an inclusive $|V_{cb}|$ determination:

$$|V_{cb}| = (41.5 \pm 0.7) \times 10^{-3} \ . \tag{27}$$

The m_b values must be quoted in the same scheme to be directly compared. For this purpose both values are translated into the shape function mass scheme, either via a second-order calculation [58,59] or via a scheme-independent physical observable [56]:

$$m_b^{SF} = 4.59 \pm 0.03\,\text{GeV} \ \text{(1S fit)}, \tag{28}$$

$$m_b^{SF} = 4.605 \pm 0.040\,\text{GeV} \ \text{(kinetic fit)}. \tag{29}$$

The m_b^{SF} values from the two fits agree well, even though the uncertainty from the two-loop scheme translation has been omitted for the 1S results. The determination of $|V_{ub}|$ discussed below uses the value from Eq. (29).

The precision of these results can be further improved. The prospects for more precise moments measurements were discussed above. Improvements can be made in the theory by calculating higher order perturbative corrections [60] and, more importantly, by calculating perturbative corrections to the matrix elements defining the HQE parameters. The inclusion of still higher order moments may improve the sensitivity of the fits to higher order terms in the HQE.

Determination of $|V_{ub}|$

Summary: The determination of $|V_{ub}|$ has improved significantly in the last year, as new measurements have become available and theoretical calculations have been improved. The determination based on inclusive semileptonic decays has an uncertainty of 8%. The dominant uncertainty (5%) comes from a 40 MeV uncertainty on m_b based on HQE fits to moments in $\overline{B} \to X_c \ell \overline{\nu}_\ell$ and $\overline{B} \to X_s \gamma$ decays. Progress has also been made in measurements of $\overline{B} \to \pi \ell \overline{\nu}_\ell$ decays; the branching fraction is now known to 8% and the partial branching fraction at high q^2 ($> 16\,\mathrm{GeV}$), the region where lattice calculations are reliable, to 14%. Further improvements in form factor calculations are needed to take advantage of this precision.

The values obtained from inclusive and exclusive determinations are consistent:

$$|V_{ub}| = (4.40 \pm 0.20 \pm 0.27) \times 10^{-3} \text{ (inclusive)}, \tag{30}$$

$$|V_{ub}| = (3.84\ ^{+0.67}_{-0.49}) \times 10^{-3} \qquad \text{(exclusive)}. \tag{31}$$

Again, the consistency may be viewed as validation, but we choose to average these values. Since in each case the dominant errors are on multiplicative factors (namely the calculated rate) we combine them weighting by relative errors to find

$$|V_{ub}| = (4.31 \pm 0.30) \times 10^{-3}\ . \tag{32}$$

$|V_{ub}|$ from inclusive decays

The theoretical description of inclusive $\overline{B} \to X_u \ell \overline{\nu}_\ell$ decays is based on the Heavy Quark Expansion, as for $\overline{B} \to X_c \ell \overline{\nu}_\ell$ decays, and leads to a predicted total decay rate with uncertainties below 5% [61,62]. Unfortunately, the total decay rate is hard to measure due to the large background from CKM-favored $\overline{B} \to X_c \ell \overline{\nu}_\ell$ transitions. Calculating the partial decay rate in regions of phase space where $\overline{B} \to X_c \ell \overline{\nu}_\ell$ decays are suppressed is more challenging, as the HQE convergence in these regions is spoiled, requiring the introduction of a non-perturbative distribution function, the "shape function" (SF) [63,64], whose form is unknown. The shape function becomes important when

the light-cone momentum component $P_+ \equiv E_X - |P_X|$ is not large compared to Λ_{QCD}. This additional difficulty can be addressed in two complementary ways. The shape function can be measured in the radiative decay $\overline{B} \to X_s\gamma$, and the results applied to the calculation of the $\overline{B} \to X_u\ell\overline{\nu}_\ell$ partial decay rate [59,65]; a great deal of theoretical activity has been focused in this area. Alternatively, measurements of $\overline{B} \to X_u\ell\overline{\nu}_\ell$ partial decay rates can be extended further into the $\overline{B} \to X_c\ell\overline{\nu}_\ell$-allowed region and consequently move closer to where the shape function becomes irrelevant and pure HQE calculations are accurate. Both of these approaches are being pursued and have begun to bear fruit.

The shape function is a universal property of B mesons at leading order. It has been recognized for over a decade [63,64] that the leading SF can be measured in $\overline{B} \to X_s\gamma$ decays. However, sub-leading shape functions [66–72] arise at each order in $1/m_b$, and differ in semileptonic and radiative B decays. The form of the shape functions cannot be calculated. Prescriptions that relate directly the partial rates for $\overline{B} \to X_s\gamma$ and $\overline{B} \to X_u\ell\overline{\nu}_\ell$ decays and thereby avoid any parameterization of the leading shape function are available [73–76]; uncertainties due to sub-leading SF remain in these approaches. Existing measurements, however, have tended to use parameterizations of the leading SF that respect constraints on the zeroth, first and second moments. At leading order the first and second moments are equal to $\overline{\Lambda} = M_B - m_b$ and μ_π^2, respectively. The relations between SF moments and the non-perturbative parameters of the HQE are known to second order in α_s [58]. As a result, measurements of HQE parameters from a variety of sources (electron energy and hadron mass moments in $\overline{B} \to X_c\ell\overline{\nu}_\ell$ decays, photon energy moments in $\overline{B} \to X_s\gamma$ decays) can now be used to constrain the SF moments, as well as provide accurate values of m_b and other parameters for use in the HQE calculation. The global fits of the HQE to $\overline{B} \to X_c\ell\overline{\nu}_\ell$ and $\overline{B} \to X_s\gamma$ moments discussed earlier have validated the application of the HQE to these distributions and provided significantly reduced parameter uncertainties. This is an important development. The possibility of measuring these

HQE parameters directly from moments in $\overline{B} \to X_u \ell \overline{\nu}_\ell$ decays is also being explored [77], although the experimental precision achievable there is not yet competitive with other approaches.

A calculation [78] of the fully differential $\overline{B} \to X_u \ell \overline{\nu}_\ell$ rate formed the basis for determinations of $|V_{ub}|$ from inclusive semileptonic decays for several years. It was based on the HQE to order $1/m_b^2$ and included $O(\alpha_s)$ corrections, followed by a simple convolution with a shape function model, and was used to calculate an acceptance fraction f_u with which the total $\overline{B} \to X_u \ell \overline{\nu}_\ell$ branching fraction and $|V_{ub}|$ were determined. This approach has some limitations. The m_b value used in the HQE calculation is not independent of the $\overline{\Lambda}$ parameter of the shape function model, but the correlation is not well determined. Furthermore, it has been noted that the simple convolution of a shape function model with the HQE is not valid beyond leading order [79,80]. An updated approach from Bosch, Lange, Neubert and Paz [59] based on SCET, hereafter referred to as "BLNP", incorporates radiative corrections to the shape function, and has been used by the Heavy Flavor Averaging Group in determining the $|V_{ub}|$ values quoted in this review.

The BLNP calculations start from the triple diffential rate using the variables

$$P_l = M_B - 2E_l, \quad P_- = E_X + |\vec{P}_X|, \quad P_+ = E_X - |\vec{P}_X| \quad (33)$$

for which the differential rate becomes

$$\frac{d^3\Gamma}{dP_+\, dP_-\, dP_l} = \frac{G_F^2 |V_{ub}|^2}{16\pi^2}(M_B - P_+) \quad (34)$$
$$\Big\{(P_- - P_l)(M_B - P_- + P_l - P_+)\mathcal{F}_1$$
$$+(M_B - P_-)(P_- - P_+)\mathcal{F}_2 + (P_- - P_l)(P_l - P_+)\mathcal{F}_3\Big\}\,.$$

The "structure functions" $\mathcal{F}_i$ can be calculated using factorization theorems that have been proven to subleading order in the $1/m_b$ expansion. These factorization theorems allow the $\mathcal{F}_i$ to be written in terms of perturbatively calculable hard coefficients H and jet functions J, which are convoluted with the (soft)

light-cone distribution functions S, the shape functions of the B Meson.

The leading order term in the $1/m_b$ expansion of the $\mathcal{F}_i$ contains a single non-perturbative function and is calculated to subleading order in α_s, while at subleading order in the $1/m_b$ expansion there are several independent non-perturbative functions which have been calculated only at tree level in the α_s expansion.

To extract the non-perturbative input one can study the photon energy spectrum in $B \to X_s\gamma$ [65]. This spectrum is known at a similar accuracy as the P_+ spectrum in $B \to X_u \ell \overline{\nu}_\ell$. Going to subleading order in the $1/m_b$ expansion requires the modeling of subleading SFs, a large variety of which were studied in [59].

Going to subleading order in α_s requires the definition of a renormalization scheme for the HQE parameters and for the shape function. It has been noted that the relation between the moments of the shape function and the forward matrix elements of local operators is plagued by ultraviolet problems which require additional renormalization. A possible scheme for improving this behavior has been suggested in Refs. [59,65], which introduce a particular definition of the quark mass (the so-called shape function scheme) based on the first moment of the measured spectrum. Likewise, the HQE parameters can be defined from measured moments of spectra, corresponding to moments of the shape function.

While attempts to measure the shape function in $\overline{B} \to X_s\gamma$ decays are important, the impact of uncertainties in the shape function is significantly reduced in some recent measurements that cover a larger portion of the $\overline{B} \to X_u \ell \overline{\nu}_\ell$ phase space. Several measurements using a combination of cuts on the leptonic momentum transfer q^2 and the hadronic invariant mass M_X as suggested in Ref. [82] have been made. Measurements of the electron spectrum in $\overline{B} \to X_u \ell \overline{\nu}_\ell$ decays have been made down to 1.9 GeV, at which point shape function uncertainties are not dominant. Direct comparisons between the partial rates calculated in the "pure" HQE and those including a model shape function are instructive. The difference in these rates

is, for many of the regions covered by existing measurements, already below 10%, suggesting that shape function uncertainties (including those from sub-leading SFs) are small. Furthermore, several of the measurements quoted below have used a variety of functional forms to parameterize the leading shape function; in no case does this lead to more than a 2% uncertainty on $|V_{ub}|$.

It has been pointed out [83,84] that Weak Annihilation (WA) can contribute significantly in the restricted region (at high q^2) accepted by measurements of $\overline{B} \to X_u \ell \overline{\nu}_\ell$ decays, and leptonic D_s decays have been used to estimate a $\sim 3\%$ uncertainty on the total $\overline{B} \to X_u \ell \overline{\nu}_\ell$ rate from the $\Upsilon(4S)$. The differential spectrum from WA decays is not well known, but they are expected to contribute predominantly in the high q^2 region, and can be a significant source of uncertainty for $|V_{ub}|$ measurements that accept only a small fraction of the total $\overline{B} \to X_u \ell \overline{\nu}_\ell$ rate. More direct experimental constraints on WA can be made by comparing the $\overline{B} \to X_u \ell \overline{\nu}_\ell$ decay rates of charged and neutral B mesons; results from such studies are not yet available. Another approach was recently explored in [85], where the CLEO data were fitted to a large range of models for WA decays, along with a spectator $\overline{B} \to X_u \ell \overline{\nu}_\ell$ component and background. An impact ratio $R = \Gamma(WA)/\Gamma(\overline{B} \to X_u \ell \overline{\nu}_\ell)$ was determined for different WA models and various analysis cuts. These estimates are used in the error analysis of BLNP.

Measurements

Progress has been made in measurements of $\overline{B} \to X_u \ell \overline{\nu}_\ell$. Large data samples and detailed studies of the charm background have allowed the momentum cut in lepton endpoint analyses to be placed well below the charm threshold; new measurements from BELLE and BABAR quote the partial rate for $\overline{B} \to X_u \ell \overline{\nu}_\ell$ decays for $E_e > 1.9$ and 2.0GeV, respectively. Other variables which allow the measurement of a large fraction of the $\overline{B} \to X_u \ell \overline{\nu}_\ell$ rate, *e.g.*, the hadron mass m_X, have been studied either with or without the reconstruction of the second B meson in the event. Given the improved precision and more rigorous theoretical interpretation of the recent measurements,

earlier determinations [86–89] of $|V_{ub}|$ will not be further considered in this review.

In all cases, the experiments need to model $\overline{B} \to X_u \ell \overline{\nu}_\ell$ decays in order to calculate acceptances and efficiencies. While theoretical expressions exist based on the partonic decay $b \to u \ell \overline{\nu}_\ell$ and quark-hadron duality, they do not incorporate any resonant structure (*e.g.* $\overline{B} \to \pi \ell \overline{\nu}_\ell$); this must be added "by hand". The uncertainties arising from this procedure for typical measurements have been estimated by the experiments to be at the level of 1-2% on $|V_{ub}|$.

The approaches used fall into three basic categories:

1. Charged lepton momentum "endpoint" measurements. In these analyses, a single charged electron is used to determine a partial decay rate for $\overline{B} \to X_u \ell \overline{\nu}_\ell$, *i.e.*, no neutrino reconstruction is employed, resulting in a $\mathcal{O}(50\%)$ selection efficiency. The decay rate can be cleanly extracted for $E_e > 2.3\,\mathrm{GeV}$, but this is deep in the SF region, where theoretical uncertainties are large. Recent measurements push down to 2.0 or 1.9 GeV, but at the cost of a low ($< 1/10$) signal-to-background (S/B) ratio.
2. Untagged "neutrino reconstruction" measurements. In this case, both the charged electron and the missing momentum are measured, allowing the determination of q^2 and providing additional background rejection. This allows a much higher S/B ~ 0.7 at the same E_e cut and a $\mathcal{O}(5\%)$ selection efficiency, but at the cost of a smaller accepted phase space for $\overline{B} \to X_u \ell \overline{\nu}_\ell$ decays and uncertainties associated with the determination of the missing momentum.
3. "Tagged" measurements in which one B meson is fully reconstructed. In this case the E_e cut is typically 1.0 GeV, and the full range of signal-side variables (q^2, M_x, P_+, etc.) is available for study. The S/B ratio can be quite high (~ 2) but the selection efficiency is $\mathcal{O}(10^{-3})$, and the impact of undetected particles from $\overline{B} \to X_c \ell \overline{\nu}_\ell$ decay (*e.g.*, K_L^0 and additional neutrinos) on the estimated background remains an important source of uncertainty.

The primary challenge in reducing the lepton momentum cut in the endpoint method is controling the $\overline{B} \to X_c \ell \overline{\nu}_\ell$ background at the required precision. In the analysis of CLEO [90], the inclusive electron momentum spectrum, after subtraction of the continuum background, was fit to a combination of a model $\overline{B} \to X_u \ell \overline{\nu}_\ell$ spectrum and components ($D\ell\overline{\nu} + D^* \ell\overline{\nu}$, $D^{**}\ell\overline{\nu}$ and non-resonant $D^{(*)}\pi\ell\overline{\nu}$) of the $\overline{B} \to X_c \ell \overline{\nu}_\ell$ spectrum. Only the normalizations of these spectra varied in the fit; uncertainties in the shapes were treated as systematic errors. BELLE [91] and BABAR [92] take similar approaches, choosing to fit for slightly different combinations of $\overline{B} \to X_c \ell \overline{\nu}_\ell$ components. The resulting partial branching fractions for various E_e cuts are given in Table 1. As expected, the leading uncertainty at the lower lepton momentum cuts comes from the $\overline{B} \to X_c \ell \overline{\nu}_\ell$ background. It should be noted that the only $\overline{B} \to X_c \ell \overline{\nu}_\ell$ decays that contribute significantly for $E_e > 2.0\,\mathrm{GeV}$ are $D\ell\overline{\nu}$ and $D^*\ell\overline{\nu}$. Reducing the lepton momentum cut further will require better knowledge of the semileptonic decays to higher mass $X_c \ell \overline{\nu}$ states. The determination of $|V_{ub}|$ from these measurements is discussed below.

An analysis from BABAR is based on the combination of a high energy electron with a measurement of the missing momentum vector [93]. The selection makes requirements on the difference between the missing energy and the magnitude of the missing momentum, and uses q^2 and E_e in the combination [94] $s_{\mathrm{h}}^{\max} = m_B^2 + q^2 - 2m_B(E_e + q^2/4E_e)$ for $\pm 2E_e > \pm\sqrt{q^2}$ and $s_{\mathrm{h}}^{\max} = m_B^2 + q^2 - 2m_B\sqrt{q^2}$ otherwise (BABAR include additional terms, omitted here, to account for the motion of the B in the $\Upsilon(4S)$ frame). No $\overline{B} \to X_c \ell \overline{\nu}_\ell$ decay can have $s_{\mathrm{h}}^{\max}$ below m_D^2 before accounting for resolution. The requirements $E_e > 2.0\,\mathrm{GeV}$ and $s_{\mathrm{h}}^{\max} < 3.5\,\mathrm{GeV}$ are imposed, resulting in an accepted fraction $f_u = 0.19$ of $\overline{B} \to X_u \ell \overline{\nu}_\ell$ decays. The quality of the neutrino reconstruction, of the modeling of the selection efficiency and of the modeling of the $\overline{B} \to X_c \ell \overline{\nu}_\ell$ background are evaluated on a sample of $\Upsilon(4S) \to B\overline{B}$ decays where one B is reconstructed as $\overline{B} \to D^0(X)e\overline{\nu}$ with $D^0 \to K^-\pi^+$ and kinematic cuts limiting the (X) to no more than a soft transition

π or γ. The partial branching fraction and $|V_{ub}|$ are given in Table 1.

The large samples accumulated at the B factories allow studies in which one B meson is fully reconstructed and the recoiling B decays semileptonically [95]. The experiments can correctly reconstruct a B candidate in about 0.5% (0.3%) of B^+B^- ($B^0\overline{B}^0$) events. An electron or muon with center-of-mass momentum above 1.0 GeV is required amongst the charged tracks not assigned to the tag B. Further requirements are imposed to reject $\overline{B} \to X_c \ell \overline{\nu}_\ell$ decays with additional missing particles. For example, the square of the missing mass is required to be consistent with zero (*e.g.,* < 0.5 GcV), and candidates with identified kaons or slow-pions from a $D^* \to D$ transition are rejected. The full set of kinematic properties (E_ℓ, M_X, q^2, *etc.*) are available for studying the semileptonically decaying B, making possible selections that accept up to 70% of the full $\overline{B} \to X_u \ell \overline{\nu}_\ell$ rate.

BELLE has measured partial rates with cuts on E_ℓ, M_X and q^2, and P_+ based on a sample of 275 million $B\overline{B}$ events [96]. The corresponding partial branching fractions are given in Table 1. As these are highly correlated measurements, only one (the most accurate, $M_X < 1.7$ GeV) is used in the average. A BABAR analysis measures the partial rate in the region $M_X < 1.7$ GeV and $q^2 > 8$ GeV based on a sample of 232 million $B\overline{B}$ events [97](see Table 1). In each case the experimental systematics have significant contributions from the modeling of $\overline{B} \to X_u \ell \overline{\nu}_\ell$ and $\overline{B} \to X_c \ell \overline{\nu}_\ell$ decays and from the detector response to charged particles, photons and neutral hadrons.

A previous BELLE analysis [98] used simulated annealing to associate particles to the semileptonic B decay and measured the partial rate with cuts on M_X and q^2, achieving higher efficiency but poorer S/B (1/6) than the tagged analyses.

Apart from the closely related measurements from Ref. [96] cited above, the statistical correlations amongst the measurements made by the same experiment are tiny (due to small overlaps among signal events and large differences in S/B ratios) and have been ignored in performing the average.

Determination of $|V_{ub}|$

The determination of $|V_{ub}|$ from the measured partial rates requires input from theory. The BLNP calculation described previously is used to determine $|V_{ub}|$ from all measured partial $\overline{B} \to X_u \ell \overline{\nu}_\ell$ rates; the values are given in Table 1. The uncertainties on the average are: statistical—2.2%; experimental—2.6%; $\overline{B} \to X_c \ell \overline{\nu}_\ell$ modeling—2.0%; $\overline{B} \to X_u \ell \overline{\nu}_\ell$ modeling—2.2%; HQE parameters (including m_b)—4.7%; subleading SFs—3.5%; Weak Annihilation—2.0%. The uncertainty on m_b dominates the uncertainty on $|V_{ub}|$ from HQE parameters; the uncertainty on $|V_{ub}|$ due to μ_π^2 is a factor of 5 or more smaller for most measurements.

Table 1: $|V_{ub}|$ from inclusive $\overline{B} \to X_u \ell \overline{\nu}_\ell$ measurements. The first uncertainty on $|V_{ub}|$ is experimental, while the second includes both theoretical ($\sim 5\%$) and HQE parameter uncertainties (the remainder). The HQE parameter input used was [56] $m_b^{SF} = 4.605 \pm 0.040$ GeV and $\mu_\pi^2(SF) = 0.20 \pm 0.04$ GeV^2.

	nominal f_u	$\lvert V_{ub}\rvert \times (10^{-3})$
*CLEO [90] $E_e > 2.1$ GeV	0.19	$4.05 \pm 0.47 \pm 0.36$
*BABAR [93] E_e, $s_{\rm h}^{\rm max}$	0.19	$4.08 \pm 0.27 \pm 0.37$
*BABAR [92] $E_e > 2.0$ GeV	0.26	$4.41 \pm 0.30 \pm 0.32$
*BELLE [91] $E_e > 1.9$ GeV	0.34	$4.85 \pm 0.45 \pm 0.31$
*BABAR [97] M_X/q^2	0.34	$4.79 \pm 0.35 \pm 0.33$
*BELLE [98] M_X/q^2	0.34	$4.41 \pm 0.46 \pm 0.30$
BELLE [96] M_X/q^2	0.34	$4.71 \pm 0.37 \pm 0.32$
BELLE [96] $P_+ < 0.66$ GeV	0.57	$4.16 \pm 0.35 \pm 0.29$
*BELLE [96] $M_X < 1.7$ GeV	0.66	$4.10 \pm 0.27 \pm 0.25$
Average of * $\chi^2 = 6.3/6$, CL=0.39		$4.40 \pm 0.20 \pm 0.27$

As was the case with $|V_{cb}|$, it is hard to assign an uncertainty to $|V_{ub}|$ for possible duality violations. Since the subleading terms in the case of $|V_{ub}|$ are much less explored, we also cannot rely on the consistency of the data and hence this remains an open issue here. On the other hand, unless duality violations are much larger in $\overline{B} \to X_u \ell \overline{\nu}_\ell$ decays than in $\overline{B} \to X_c \ell \overline{\nu}_\ell$

decays, the precision of the $|V_{ub}|$ determination is not yet at the level where duality violations are likely to be significant. If one proceeds along the lines suggested in Ref. [81], an ad-hoc estimate for the uncertainty from potential duality violations can be obtained using the set of measurements in Table 1. Fitting those measurements to a function of f_u under the assumption that duality violations scale as $(1 - f_u)/f_u$, the resulting bias is $-2.0 \pm 4.3\%$ relative to the assumption of no duality violations. This is consistent with the uncertainty from duality violation being small; we do not consider it appropriate to add this uncertainty to the average.

An independent calculation by Bauer, Ligeti and Luke [82] is available for the case of cuts on M_X and q^2. Using the same input for m_b, translated into the 1S scheme, yields a $|V_{ub}|$ value 3.5% larger than obtained with BLNP; this is within the quoted theory error.

HQE parameters and shape function input

The global fits to $\overline{B} \to X_c \ell \overline{\nu}_\ell$ moments discussed earlier provide input values for the heavy quark parameters needed in calculating $\overline{B} \to X_u \ell \overline{\nu}_\ell$ partial rates. These HQE parameters are also used to constrain the first and second moments of the shape function. Additional information on the leading shape function and HQE parameters is obtained from the photon energy spectrum in $\overline{B} \to X_s \gamma$ decays. There are two means of extracting information from the spectrum; fitting the full spectrum using a functional ansatz for the shape function, or determining the low-order moments above a threshold energy cut.

BELLE, BABAR and CLEO have measured the $\overline{B} \to X_s \gamma$ spectrum and its moments [49–52] down to $E_\gamma = 1.8\,\mathrm{GeV}$, $1.9\,\mathrm{GeV}$ and $2.0\,\mathrm{GeV}$, respectively. The experimental data are most precise at the very highest photon energies where the background, especially from B decays, is smallest. In most analyses the photon energy is measured in the $\Upsilon(4S)$ rest frame, which produces a significant smearing of the spectrum. One of the BABAR analyses [50], based on the sum of $\overline{B} \to X_s \gamma$ exclusive states involving a kaon and up to 4 pions, avoids this smearing by using the measured invariant mass of

the recoiling hadron as the observable, resulting in excellent E_γ resolution in the B rest frame. This analysis shows a clear K^* peak near the endpoint of the photon spectrum, and highlights the issue of how sensitive a fit to the full spectrum is to local quark-hadron duality (even when lumping the K^* region into a single bin). In addition, the form of the shape function is unknown; multiple functional ansatze must be employed to estimate the uncertainty arising from this model dependence.

Fits to the full $\overline{B} \to X_s\gamma$ spectrum have been performed using the calculation of Ref. [99], which includes the NLO relations between the spectra of $b \to s\gamma$ and $b \to u\ell\overline{\nu}_\ell$ in the shape function scheme and is an improvement on earlier work [100]. A recent fit from BABAR gives [50] $m_b^{SF} = 4.67 \pm 0.07\,\mathrm{GeV}$; if instead they take the same data and fit the first and second moments of the E_γ spectrum for $E_\gamma > 1.897\mathrm{GeV}$ they find $m_b^{SF} = 4.60^{+0.12}_{-0.14}\,\mathrm{GeV}$. BELLE determines [103] $m_b^{SF} = 4.52 \pm 0.07\,\mathrm{GeV}$ from a fit to their spectrum.

Another theoretical approach using "dressed gluon exponentiation" has recently become available for calculating decay spectra for $\overline{B} \to X_s\gamma$ and $\overline{B} \to X_u\ell\overline{\nu}_\ell$ [104].

Predictions of the photon energy moments in terms of HQE parameters are available in several mass renormalization schemes and several approaches [60, 101, 102]. The predicted moments at low photon energy cuts (*e.g.* $E_\gamma > 1.6$ GeV) are insensitive to shape function uncertainties. For cuts of ~ 1.8 GeV, corrections [105] need to be applied, and the associated theoretical uncertainty becomes sizable for cuts above ~ 2.0 GeV. The experimental accuracy on the truncated moments is best at high E_γ cuts and degrades significantly at lower cuts due to large backgrounds. In a compromise between these two sources of uncertainty, the global HQE fits discussed earlier use moments at E_γ cuts up to 2.0 or 2.1 GeV, and include an estimate of the theoretical uncertainty from SF effects.

Status and outlook

At present, as indicated by the average given above, the uncertainty on $|V_{ub}|$ is at the 8% level. The uncertainty on m_b taken here is 40 MeV, contributing an uncertainty of 4.5% on $|V_{ub}|$; reducing this further will be increasingly difficult due to

theoretical uncertainties in the determination of m_b from the global fits to moments. However, further progress can be expected on some of the other leading sources of uncertainty. The uncertainties on $|V_{ub}|$ quoted in the BLNP calculation are at the 5% level. The Weak Annihilation component of this can be better addressed experimentally at the B factories. Reducing the remaining theory uncertainty will require improvements in the calculations. For the approaches making use of the shape function this amounts to improvements in relating the spectra from $\overline{B} \to X_u \ell \overline{\nu}_\ell$ and $\overline{B} \to X_s \gamma$ decays by calculating radiative corrections and the effects of subleading shape functions, while approaches less sensitive to shape functions require calculations of higher-order radiative corrections. Experimental uncertainties will be reduced through higher statistics and better understanding of $\overline{B} \to X_c \ell \overline{\nu}_\ell$ decays and of D decays. The two approaches discussed earlier, namely (1) determining the shape function from the $\overline{B} \to X_s \gamma$ photon spectrum and applying it to $\overline{B} \to X_u \ell \overline{\nu}_\ell$ decays and (2) pushing the measurements into regions where shape function and duality uncertainties become negligeable, are fairly complementary and should both be pursued.

$|V_{ub}|$ from exclusive decays

Exclusive charmless semileptonic decays offer a complementary means of determining $|V_{ub}|$. For the experiments, the specification of the final state provides better background rejection, but the lower branching fraction reflects itself in lower yields compared with inclusive decays. For theory, the calculation of the form factors for $\overline{B} \to X_u \ell \overline{\nu}_\ell$ decays is challenging, but brings in a different set of uncertainties from those encountered in inclusive decays. In this review we focus on $\overline{B} \to \pi \ell \overline{\nu}_\ell$, as it is the most promising mode for both experiment and theory, and recent improvements have been made in both areas. Measurements of other exclusive states can be found in Refs. [107–111].

$\overline{B} \to \pi \ell \overline{\nu}_\ell$ form factor calculations The relevant form factors for the decay $\overline{B} \to \pi \ell \overline{\nu}_\ell$ are usually defined as

$$\langle\pi(p_\pi)|V^\mu|B(p_B)\rangle = \tag{35}$$
$$f_+(q^2)\left[p_B^\mu + p_\pi^\mu - \frac{m_B^2 - m_\pi^2}{q^2}q^\mu\right] + f_0(q^2)\frac{m_B^2 - m_\pi^2}{q^2}q^\mu$$

in terms of which the rate becomes (in the limit $m_\ell \to 0$)

$$\frac{d\Gamma}{dq^2} = \frac{G_F^2|V_{ub}|^2}{24\pi^3}|p_\pi|^3|f_+(q^2)|^2 \tag{36}$$

where p_π is the momentum of pion in the B meson rest frame.

Currently available non-perturbative methods for the calculation of the form factors include lattice QCD and light-cone sum rules. The two methods are complementary in phase space, since the lattice calculation is restricted to the kinematical range of high momentum transfer q^2 to the leptons, due to large discretization errors, while light-cone sum rules provide information near $q^2 = 0$. Interpolations between these two regions may be constrained by unitarity and analyticity.

Unquenched simulations, for which quark loop effects in the QCD vacuum are fully incorporated, have become quite common, and the first results based on these simulations for the $\overline{B} \to \pi\ell\overline{\nu}_\ell$ form factors have been obtained recently by the Fermilab/MILC collaboration [112] and the HPQCD collaboration [113].

The two calculations differ in the way the b quark is simulated, with HPQCD using nonrelativistic QCD and Fermilab/MILC the so-called Fermilab heavy quark method. Results by the two groups for $f_0(q^2)$ and $f_+(q^2)$ are shown in Fig. 3. The two calculations agree within the quoted errors.

In order to obtain the partially-integrated differential rate, the BK parameterization [114]

$$f_+(q^2) = \frac{c_B(1-\alpha_B)}{(1-\tilde{q}^2)(1-\alpha_B\tilde{q}^2)}, \tag{37}$$
$$f_0(q^2) = \frac{c_B(1-\alpha_B)}{(1-\tilde{q}^2/\beta_B)}, \tag{38}$$

with $\tilde{q}^2 \equiv q^2/m_{B^*}^2$ is used to extrapolate to small values of q^2. It includes the leading pole contribution from B^*, and

higher poles are modeled by a single pole. The heavy quark scaling is satisfied if the parameters c_B, α_B and β_B scale appropriately. However, the BK parameterization should be used with some caution, since it is not consistent with SCET [115]. Alternatively, one may use analyticity and unitarity bounds to constrain the form factors. The use of lattice data in combination with a data point at small q^2 from SCET or sum rules provides a stringent constraint on the shape of the form factor [116].

The results for the integrated rate with $q^2 > q^2_{\rm cut} = 16{\rm GeV}^2$ are

$$\begin{aligned} \Gamma &= |V_{ub}|^2 \times (1.31 \pm 0.33)\,{\rm ps}^{-1}, \qquad \text{HPQCD;} \\ &= |V_{ub}|^2 \times (1.80 \pm 0.48)\,{\rm ps}^{-1}, \qquad \text{Fermilab/MILC.} \end{aligned}$$

Here the statistical and systematic errors are added in quadrature.

Much work remains to be done, since the current combined statistical plus systematic errors in the lattice results are still at the 10-14% level on $|V_{ub}|$ and need to be reduced. Reduction of errors to the $5 \sim 6\%$ level for $|V_{ub}|$ may be feasible within the next few years, although that could involve carrying out a two-loop (or fully non-perturbative) matching between lattice and continuum QCD heavy-to-light current operators, and/or going to smaller lattice spacing.

Another established non-perturbative approach to obtain the form factors is through Light-Cone QCD Sum Rules (LCSR), although some skepticism has been expressed from the point of view of SCET [117]. The sum-rule approach provides an approximation for the product $f_B f_+(q^2)$, valid in the region $0 < q^2 <\sim 14\,{\rm GeV}^2$. The determination of $f_+(q^2)$ itself requires knowledge of the decay constant f_B, which usually is obtained by replacing f_B by its two-point QCD (SVZ) sum rule [118] in terms of perturbative and condensate contributions. The advantage of this procedure is the approximate cancellation of various theoretical uncertainties in the ratio $(f_B f_+)/(f_B)$. The LCSR for $f_B f_+$ is based on the light-cone OPE of the relevant vacuum-to-pion correlation function, calculated in full

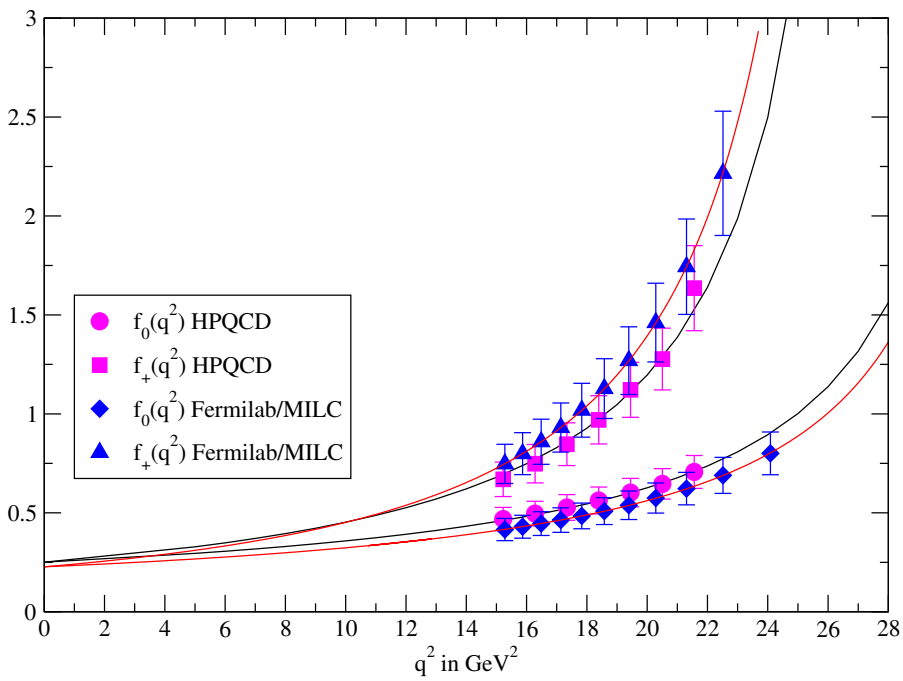

Figure 3: The form factors $f_0(q^2)$ and $f_+(q^2)$ versus q^2 by the Fermilab/MILC [112] and HPQCD [113] collaborations. The full curves are the BK parameterization [114] fits to the simulation results at large q^2, with $f_0(0)$ and $f_+(0)$ constrained to be equal. Errors are statisical plus systematic added in quadrature.

QCD at finite b-quark mass. The resulting expressions actually comprise a triple expansion: in the twist t of the operators near the light-cone, in α_s, and in the deviation of the pion distribution amplitudes from their asymptotic form, which is fixed from conformal symmetry.

After identifying all sources of uncertainties in LCSR, the updated analysis of [119](see also [120]) gives the following value

$$f_+(0) = 0.27\Big[1 \pm (5\%)_{tw>4} \pm (3\%)_{m_b,\mu} \pm (3\%)_{\langle\bar{q}q\rangle} \pm (3\%)_{s_0^B,M} \pm (8\%)_{a^\pi_{2,4}}\Big]\,, \tag{39}$$

where the uncertainties are displayed individually. Here s_0^B, M labels the uncertainty estimated from the use of the sum rule (threshold and Borel parameters) and $a_{2,4}^{\pi}$ labels the uncertainty due to non-asymptotic contributions of the pion distribution amplitude.

Combining the uncertainties one obtains

$$f_+(0) = 0.27 \pm 0.04\,, \tag{40}$$

where the first four uncertainties are combined in quadrature and the last uncertainty is added linearily. This value is consistent with the value quoted in [121]

$$f_+(0) = 0.258 \pm 0.031 \tag{41}$$

It is interesting to note that the results from the LQCD and LCSR are consistent with each other when the BK parameterization is used to relate them. This increases confidence in the theoretical predictions for the rate of $\overline{B} \to \pi \ell \overline{\nu}_\ell$.

An alternative determination of $|V_{ub}|$ has been proposed by several authors [122–126]. It is based on a model-independent relation between rare decays such as $\overline{B} \to K^* \ell^+ \ell^-$ and $\overline{B} \to \rho \ell \overline{\nu}_\ell$, which can be obtained at large momentum transfer q to the leptons. This method is based on the HQET relations between the matrix elements of the $B \to K^*$ and the $B \to \rho$ transitions and a systematic, OPE-based expansion in powers of m_c^2/q^2 and $\Lambda_{\rm QCD}/q$. The theoretical uncertainty is claimed to be of the order of 5% for $|V_{ub}|$; however, it requires a precise measurement of the exclusive rare decay $\overline{B} \to K^* \ell^+ \ell^-$, which is a task for future ultra-high-rate experiments.

$\overline{B} \to \pi \ell \overline{\nu}_\ell$ measurements

The $\overline{B} \to \pi \ell \overline{\nu}_\ell$ measurements fall into two broad classes: untagged, in which case the reconstruction of the missing momentum of the event serves as an estimator for the unseen neutrino, and tagged, in which the second B meson in the event is fully reconstructed in either a hadronic or semileptonic decay mode. The tagged measurements have high and uniform acceptance, S/B ~ 3, but low statistics. The untagged measurements have somewhat higher background levels (S/B ~ 1) and make

slightly more restrictive kinematic cuts, but offer large-enough statistics to be sensitive to the q^2 dependence of the form factor. The averages of the full and partial branching fractions from the tagged measurements are currently of comparable precision to the corresponding averages of the untagged measurements.

Table 2: Total and partial branching fractions for $\overline{B}^0 \to \pi^+\ell^-\overline{\nu}_\ell$. The uncertainties are from statistics and systematics. The measurements of $\mathcal{B}(B^- \to \pi^0\ell^-\overline{\nu}_\ell)$ have been multiplied by a scale factor $2\tau_{B^0}/\tau_{B^+}$ to obtain the value quoted below. The confidence level of the total branching fraction average is 0.33.

	$\mathcal{B}\times 10^4$	$\mathcal{B}(q^2 > 16) \times 10^4$
CLEO π^+, π^0 [110]	$1.32 \pm 0.18 \pm 0.13$	$0.25 \pm 0.09 \pm 0.05$
BABAR π^+, π^0 [111]	$1.38 \pm 0.10 \pm 0.18$	$0.49 \pm 0.05 \pm 0.06$
Average of untagged	$1.35 \pm 0.10 \pm 0.14$	$0.41 \pm 0.04 \pm 0.05$
BELLE SL π^+ [128]	$1.48 \pm 0.20 \pm 0.16$	$0.40 \pm 0.12 \pm 0.05$
BELLE SL π^0 [128]	$1.40 \pm 0.24 \pm 0.16$	$0.41 \pm 0.15 \pm 0.04$
BABAR SL π^+ [130]	$1.02 \pm 0.25 \pm 0.13$	$0.21 \pm 0.14 \pm 0.05$
BABAR SL π^0 [131]	$3.31 \pm 0.68 \pm 0.42$	NA
BABAR had π^+ [132]	$1.24 \pm 0.29 \pm 0.16$	$0.70 \pm 0.22 \pm 0.11$
BABAR had π^0 [132]	$1.45 \pm 0.37 \pm 0.12$	$0.46 \pm 0.20 \pm 0.04$
Average of tagged	$1.36 \pm 0.11 \pm 0.08$	$0.39 \pm 0.07 \pm 0.03$
Average	$1.35 \pm 0.08 \pm 0.08$	$0.40 \pm 0.04 \pm 0.04$

CLEO has analyzed $\overline{B} \to \pi\ell\overline{\nu}_\ell$ and $\overline{B} \to \rho\ell\overline{\nu}_\ell$ using an untagged analysis [110]. A similar analysis has been done by BABAR [111]. The measured q^2 dependence favors QCD-inspired form factor calculations (lattice or LCSR) over the widely used ISGW2 [127] model. The leading systematic uncertainties in the untagged $\overline{B} \to \pi\ell\overline{\nu}_\ell$ analyses are associated with modeling the missing momentum reconstruction and with varying the form factor for the $\overline{B} \to \rho\ell\overline{\nu}_\ell$ decay, which is a major source of background. The values obtained for the full and partial branching fractions are listed in Table 2.

BELLE has performed an analysis based on reconstructing a B^0 in the $D^{(*)-}\ell^+\nu_\ell$ decay mode and looking for a $\overline{B}^0 \to$

$\pi^+\ell^-\overline{\nu}_\ell$ or $\overline{B}^0 \to \rho^+\ell\overline{\nu}_\ell$ decay amongst the remaining particles in the event; the most recent Belle results are given in Ref. [128]. The fact that the B and $\overline{B}$ are back-to-back in the $\Upsilon(4S)$ frame is used to construct a discriminating variable and obtain a signal-to-noise ratio above unity for all q^2 bins. A related technique was discussed in Ref. [129]. BABAR has done similar analyses [130,131] in the $\overline{B}^0 \to \pi^+\ell^-\overline{\nu}_\ell$ and $B^- \to \pi^0\ell^-\overline{\nu}_\ell$ channels, where in the latter case the tagging decays are $B^+ \to \overline{D}^0\ell^+\nu(X)$ and kinematic requirements accept decays to $\overline{D}^{*0}\ell^+\nu$ where the π^0 or γ from the $\overline{D}^{*0} \to \overline{D}^0$ transition is unreconstructed. In addition, the sample of fully-reconstructed B mesons in BABAR has been used to measure exclusive charmless semileptonic decays [132], giving very clean but low-yield samples. The resulting full and partial branching fractions are given in Table 2.

The outlook for improvements in these measurements with increasing B-factory data samples is good. The tagged measurements in particular will improve; the current estimates of systematic uncertainties in these measurements have a significant statistical component, so the total experimental uncertainty should fall as $1/\sqrt{N}$ for some time.

Table 3: Determinations of $|V_{ub}|$ based on $\overline{B} \to \pi\ell\overline{\nu}_\ell$ decays.

Method	$\lvert V_{ub}\rvert \times (10^{-3})$
LCSR, [121] full q^2	$3.37 \pm 0.14^{+0.66}_{-0.41}$
LCSR, [121] $q^2 < 16$	$3.27 \pm 0.16^{+0.54}_{-0.36}$
HPQCD, [113] full q^2	$3.93 \pm 0.17^{+0.77}_{-0.48}$
HPQCD, [113] $q^2 > 16$	$4.47 \pm 0.30^{+0.67}_{-0.46}$
FNAL, [112] full q^2	$3.76 \pm 0.16^{+0.87}_{-0.51}$
FNAL, [112] $q^2 > 16$	$3.78 \pm 0.25^{+0.65}_{-0.43}$

Table 3 shows the $|V_{ub}|$ values obtained based on form factor calculations from QCD sum rules and lattice QCD. We quote an average based on three inputs: the measured partial branching fractions in the region $q^2 > 16$ GeV^2 with theory input from the two unquenched lattice calculations, and the

partial branching fractions in the region $q^2 < 16$ GeV^2 with theory input from LCSR. The uncertainty on the theory input is large compared to the uncertainty from the measurements. We form the arithmetic averages of the values and of the errors to find

$$|V_{ub}| = (3.84\ ^{+0.67}_{-0.49}) \times 10^{-3}\ . \tag{42}$$

The uncertainty is dominated by the form factor normalization, the calculations of which were discussed previously.

Conclusion

The study of semileptonic B meson decays continues to be an active area for both theory and experiment. Substantial progress has been made in the application of HQE calculations to inclusive decays, with fits to moments of $\overline{B} \to X_c \ell \overline{\nu}_\ell$ and $B \to X_s \gamma$ decays providing precise values for $|V_{cb}|$ and m_b. In particular, the precision on $|V_{cb}|$ now approaches that of the Cabibbo angle, underlining the fantastic progress made in this area. Furthermore, the consistency of the values extracted from exclusive and inclusive measurements gives us confidence, since the theoretical and experimental approaches are completely uncorrelated.

Improved measurements of $\overline{B} \to X_u \ell \overline{\nu}_\ell$ decays, along with a more comprehensive theoretical treatment and improved knowledge of m_b, have led to a significantly more precise determination of $|V_{ub}|$. Further progress in these areas is possible, but will require higher order radiative corrections from the theory and, in the case of $|V_{ub}|$, improved experimental knowledge of the $\overline{B} \to X_c \ell \overline{\nu}_\ell$ background. While there has been impressive progress in the past few years, new challenges will need to be overcome to achieve a precision below 5% on $|V_{ub}|$ from inclusive decays.

Progress in both $b \to u$ and $b \to c$ exclusive channels depends crucially on progress in lattice calculations. Here the prospects are rosy (see, *e.g.*, Ref. [133]), since unquenched lattice simulations are now possible, although the ultimate attainable precision is hard to estimate.

The measurements of $\overline{B} \to \pi \ell \overline{\nu}_\ell$ have improved significantly, and high-purity tagged measurements now provide a precision comparable to the one from untagged measurements. The experimental input will continue to improve as B-factory data sets increase. Reducing the theoretical uncertainties to a comparable level will require significant effort, but is clearly vital in order to compare the extracted $|V_{ub}|$ with the one obtained from inclusive decays.

Both $|V_{cb}|$ and $|V_{ub}|$ are indispensable inputs into unitarity triangle fits. In particular, knowing $|V_{ub}|$ with a precision of better than 10% allows a test CKM unitarity in the most direct way, by comparing the length of the $|V_{ub}|$ side of the unitarity triangle, with the measurement of $\sin(2\beta)$. This is a comparison of a "tree" process ($b \to u$) with a "loop-induced" process ($B^0 - \overline{B}^0$ mixing), and provides sensitivity to possible contributions from new physics. While the effort required to further improve our knowledge of these CKM matrix elements is large, it is well motivated.

The authors would like to acknowledge helpful discussions with M. Artuso, E. Barberio, C. Bauer, I. I. Bigi, L. Gibbons, A. Kronfeld, Z. Ligeti, V. Luth, M. Neubert and S. Stone.

References

1. See M. Artuso and E. Barberio, Phys. Lett. **B592**, 786 (2004).
2. See M. Battaglia and L. Gibbons, Phys. Lett. **B592**, 793 (2004).
3. Report from the Heavy Flavor Averaging Group, to appear in `hep-ex`.
4. N. Isgur and M.B. Wise, Phys. Lett. **B232**, 113 (1989); *ibid.* **B237**, 527 (1990).
5. M.A. Shifman and M.B. Voloshin, Sov. J. Nucl. Phys. **47**, 511 (1988) [Yad. Fiz. **47**, 801 (1988)].
6. M.E. Luke, Phys. Lett. **B252**, 447 (1990).
7. M. Ademollo and R. Gatto, Phys. Rev. Lett. **13**, 264 (1964).
8. A.V. Manohar and M.B. Wise, Camb. Monogr. Part. Phys. Nucl. Phys. Cosmol. **10**,1(2000).
9. B. Grinstein, Nucl. Phys. **B339**, 253 (1990);
   H. Georgi, Phys. Lett. **B240**, 447 (1990);

A.F. Falk *et al.*, Nucl. Phys. **B343**, 1 (1990);
E. Eichten and B. Hill, Phys. Lett. **B234**, 511 (1990).

10. A. Sirlin, Nucl. Phys. **B196**, 83 (1982).
11. A. Czarnecki and K. Melnikov, Nucl. Phys. **B505**, 65 (1997).
12. C.G. Boyd *et al.*, Phys. Rev. **D56**, 6895 (1997).
13. I. Caprini *et al.*, Nucl. Phys. **B530**, 153 (1998).
14. S. Hashimoto *et al.*, Phys. Rev. **D66**, 014503 (2002).
15. D. Buskulic *et al.*, Phys. Lett. **B395**, 373 (1997).
16. G. Abbiendi *et al.*, Phys. Lett. **B482**, 15 (2000).
17. P. Abreu *et al.*, Phys. Lett. **B510**, 55 (2001).
18. J. Abdallah *et al.*, Eur. Phys. J. **C33**, 213 (2004).
19. K. Abe *et al.*, Phys. Lett. **B526**, 247 (2002).
20. N.E. Adam *et al.*, Phys. Rev. **D67**, 032001 (2003).
21. B. Aubert *et al.*, (BABAR Collab.), `hep-ex/0408027`.
22. N. Uraltsev, Phys. Lett. **B585**, 253 (2004).
23. A. Kronfeld, talk presented at the workshop CKM05, San Diego, CA - Workshop on the Unitarity Triangle, 15-18 March 2005.
24. S. Hashimoto *et al.*, Phys. Rev. **D61**, 014502 (2000).
25. A.S. Kronfeld, Phys. Rev. **D62**, 014505 (2000).
26. J. Harada *et al.*, Phys. Rev. **D65**, 094513 (2002).
27. J. Harada *et al.*, Phys. Rev. **D65**, 094514 (2002).
28. A.S. Kronfeld, Nucl. Phys. (Proc. Supp.) **B129**, 46 (2004).
29. M. A. Nobes and H. D. Trottier, Nucl. Phys. (Proc. Supp.) **B129**, 355 (2004).
30. M.B. Oktay *et al.*, Nucl. Phys. (Proc. Supp.) **B129**, 349 (2004).
31. A.V. Manohar and M.B. Wise, Phys. Rev. **D49**, 1310 (1994).
32. I.I.Y. Bigi *et al.*, Phys. Rev. Lett. **71**, 496 (1993), Phys. Lett. **B323**, 408 (1994).
33. M.A. Shifman, `hep-ph/0009131`, I.I.Y. Bigi and N. Uraltsev, Int. J. Mod. Phys. **A16**, 5201 (2001).
34. D. Benson *et al.*, Nucl. Phys. **B665**, 367 (2003).
35. I.I.Y. Bigi *et al.*, Phys. Rev. **D56**, 4017 (1997).
36. I.I.Y. Bigi *et al.*, Phys. Rev. **D52**, 196 (1995).
37. A.H. Hoang *et al.*, Phys. Rev. **D59**, 074017 (1999).
38. H. Jeutwyler, Phys. Lett. **B98**, 447 (1981);

M.B. Voloshin, Sov. J. Nucl. Phys. **36**, 143 (1982).

39. C.W. Bauer *et al.*, Phys. Rev. **D70**, 094017 (2004).
40. S.E. Csorna *et al.*, (CLEO Collab.), Phys. Rev. **D70**, 032002 (2004).
41. A.H. Mahmood *et al.*, (CLEO Collab.), Phys. Rev. **D70**, 032003 (2004).
42. B. Aubert *et al.*, (BABAR Collab.), Phys. Rev. **D69**, 111103 (2004).
43. B. Aubert *et al.*, (BABAR Collab.), Phys. Rev. **D69**, 111104 (2003).
44. B. Aubert *et al.*, (BABAR Collab.), Phys. Rev. Lett. **93**, 011803 (2004).
45. K. Abe *et al.*(BELLE Collab.), `hep-ex/0408139`;
    K. Abe *et al.*(BELLE Collab.), `hep-ex/0509013`.
46. K. Abe *et al.*(BELLE Collab.), `hep-ex/0409015`;
    K. Abe *et al.*(BELLE Collab.), `hep-ex/0508056`.
47. J. Abdallah *et al.*, (DELPHI Collab.), CERN-PH-EP/2005-015 (2005).
48. D. Acosta *et al.*, (CDF Collab.), Phys. Rev. **D71**, 051103 (2005).
49. P. Koppenburg *et al.*, (BELLE Collab.), Phys. Rev. Lett. **93**, 061803 (2004);
    K. Abe *et al.*, (BELLE Collab.), `hep-ex/0508005`.
50. B. Aubert *et al.*, (BABAR Collab.), `hep-ex/050800`.
51. B. Aubert *et al.*, (BABAR Collab.), `hep-ex/0507001`.
52. S. Chen *et al.*, (CLEO Collab.), Phys. Rev. Lett. **87**, 251807 (2001).
53. M. Battaglia *et al.*, Phys. Lett. **B556**, 41 (2003).
54. B. Aubert *et al.*, (BaBar Collab.), Phys. Rev. Lett. **93**, 011803 (2004).
55. C. W. Bauer *et al.*, Phys. Rev. **D70**, 094017 (2004).
56. O. Buchmüller and H. Flächer, `hep-ph/0507253`.
57. K. Melnikov and A. Yelkhovsky, Phys. Rev. **D59**, 114009 (1999).
58. M. Neubert, Phys. Lett. **B612**, 13 (2005).
59. B.O. Lange, M. Neubert, and G. Paz, `hep-ph/0504071`.
60. M. Neubert, `hep-ph/0506245`.
61. A. H. Hoang *et al.*, Phys. Rev. **D59**, 074017 (1999).
62. N. Uraltsev, Int. J. Mod. Phys. **A14**, 4641 (1999).
63. M. Neubert, Phys. Rev. **D49**, 4623 (1994); *ibid.* **D49**, 3392 (1994).

64. I. Bigi *et al.*, Int. J. Mod. Phys. **A9**, 2467 (1994).
65. T. Mannel and S. Recksiegel, Phys. Rev. **D60**, 114040 (1999).
66. C. W. Bauer *et al.*, Phys. Rev. **D68**, 094001 (2003).
67. C. W. Bauer *et al.*, Phys. Lett. **B543**, 261 (2002).
68. S. W. Bosch *et al.*, JHEP **0411**, 073 (2004).
69. A. W. Leibovich *et al.*, Phys. Lett. **B539**, 242 (2002).
70. M. Neubert, Phys. Lett. **B543**, 269 (2002).
71. K. S. M. Lee and I. W. Stewart, Nucl. Phys. **B721**, 325 (2005).
72. M. Beneke *et al.*, JHEP **0506**, 071 (2005).
73. M. Neubert, Phys. Lett. **B543**, 269 (2002).
74. A. K. Leibovich *et al.*, Phys. Rev. **D61**, 053006 (2000); Phys. Lett. **B513**, 83 (2001).
75. A.H. Hoang *et al.*, Phys. Rev. **D71**, 093007 (2005).
76. B. Lange *et al.*, `hep-ph/0508178`.
77. P. Gambino *et al.*, `hep-ph/0505091`.
78. F. De Fazio and M. Neubert, JHEP **06**, 017 (1999).
79. C. W. Bauer and A. Manohar, Phys. Rev. **D70**, 034024 (2004).
80. S. W. Bosch *et al.*, Nucl. Phys. **B699**, 355 (2004).
81. L. Gibbons, AIP Conf. Proc. **722**, 156 (2004).
82. C. W. Bauer *et al.*, Phys. Rev. **D64**, 113004 (2001); Phys. Lett. **B479**, 395 (2000).
83. I. I. Y. Bigi and N. G. Uraltsev, Nucl. Phys. **B423**, 33 (1994).
84. M.B. Voloshin, Phys. Lett. **B515**, 74 (2001).
85. Tom Meyer, "Limits on weak annihilation in inclusive charmless semileptonic B decays," Ph.D. thesis, Cornell University (2005)..
86. R. Barate *et al.*, (ALEPH Collab.), Eur. Phys. J. **C6**, 555 (1999).
87. M. Acciarri *et al.*, (L3 Collab.), Phys. Lett. **B436**, 174 (1998).
88. G. Abbiendi *et al.*, (OPAL Collab.), Eur. Phys. J. **C21**, 399 (2001).
89. P. Abreu *et al.*, (DELPHI Collab.), Phys. Lett. **B478**, 14 (2000).
90. A. Bornheim *et al.*, (CLEO Collab.), Phys. Rev. Lett. **88**, 231803 (2002).

91. A. Limosani *et al.*, (BELLE Collab.), Phys. Lett. **B621**, 28 (2005).
92. B. Aubert *et al.*, (BABAR Collab.), `hep-ex/0509040`.
93. B. Aubert *et al.*, (BABAR Collab.), Phys. Rev. Lett. **95**, 111801 (2005).
94. R. Kowalewski and S. Menke, Phys. Lett. **B541**, 29 (2002).
95. B. Aubert *et al.*, (BABAR Collab.), Phys. Rev. Lett. **92**, 071802 (2004).
96. I. Bizjak *et al.*, (BELLE Collab.), `hep-ex/0505088`.
97. B. Aubert *et al.*(BABAR Collab.), `hep-ex/0507017`.
98. H. Kakuno *et al.*, (BELLE Collab.), Phys. Rev. Lett. **92**, 101801 (2004).
99. M. Neubert, Eur. Phys. J. **C40**, 165-186 (2005).
100. A.L. Kagan and M. Neubert, Eur. Phys. J. **C7**, 5 (1999).
101. D. Benson *et al.*, Nucl. Phys. **B710**, 371-401 (2005).
102. Z. Ligeti *et al.*, Phys. Rev. **D60**, 034019 (1999); C. Bauer, Phys. Rev. **D57**, 5611 (1998); Erratum-*ibid.* **D60**,099907(1999).
103. A. Limosani and T. Nozaki, `hep-ex/0407052`; I. Bizjak *et al.*, `hep-ex/0506057`.
104. E. Gardi, JHEP **0404**, 049 (2004); *ibid.* **0502**, 053 (2005); J.R. Andersen and E. Gardi, JHEP **0506**, 030 (2005).
105. I. I. Bigi and N. Uraltsev, Phys. Lett. **B579**, 340 (2004).
106. K. Benslama *et al.*, (CLEO-c/CESR-c Taskforces and CLEO Collab.), `hep-ex/0205003`.
107. B. H. Behrens *et al.*, (CLEO Collab.), Phys. Rev. **D61**, 052001 (2000).
108. B. Aubert *et al.*, (BABAR Collab.), Phys. Rev. Lett. **90**, 181801 (2003).
109. K. Abe *et al.*, (BELLE Collab.), Phys. Rev. Lett. **93**, 131803 (2004).
110. S. B. Athar *et al.*, (CLEO Collab.), Phys. Rev. **D68**, 072003 (2003).
111. B. Aubert *et al.*(BABAR Collab.), `hep-ex/0507003` .
112. M. Okamoto *et al.*, (Fermilab/MILC), Nucl. Phys. (Proc. Supp.) **B140**, 461 (2005).
113. J. Shigemitsu *et al.*, (HPQCD), Nucl. Phys. (Proc. Supp.) **B140**, 464 (2005).
114. D. Becirevic and A. B. Kaidalov, Phys. Lett. **B478**, 417 (2000).

115. T. Becher and R. J. Hill, hep-ph/0509090.
116. M. C. Arnesen *et al.*, Phys. Rev. Lett. **95**, 071802 (2005).
117. T. Hurth *et al.*, hep-ph/0509167.
118. M. A. Shifman, A. I. Vainshtein, and V. I. Zakharov, Nucl. Phys. **B147**, 385 (1979); *ibid.* **B147**, 448 (1979).
119. A. Khodjamirian *et al.*, Phys. Rev. **D62**, 114002 (2000).
120. M. Battaglia *et al.*, hep-ph/0304132.
121. P. Ball and R. Zwicky, Phys. Rev. **D71**, 014015 (2005).
122. N. Isgur and M.B. Wise, Phys. Rev. **D42**, 2388 (1990).
123. A.I. Sanda and A. Yamada, Phys. Rev. Lett. **75**, 2807 (1995).
124. Z. Ligeti and M.B. Wise, Phys. Rev. **D53**, 4937 (1996).
125. Z. Ligeti *et al.*, Phys. Lett. **B420**, 359 (1998).
126. B. Grinstein and D. Pirjol, Phys. Rev. **D70**, 114005 (2004).
127. D. Scora and N. Isgur, Phys. Rev. **D52**, 2783 (1995).
128. BELLE Collab., hep-ex/0508018.
129. W. Brower and H. Paar, Nucl. Instrum. Methods **A421**, 411 (1999).
130. B. Aubert *et al.*, (BABAR Collab.), hep-ex/0506064.
131. B. Aubert *et al.*, (BABAR Collab.), hep-ex/0506065.
132. B. Aubert *et al.*, (BABAR Collab.), hep-ex/0408068.
133. C. T. H. Davies *et al.*, (HPQCD, MILC and Fermilab Lattice Collab.), Phys. Rev. Lett. **92**, 022001 (2004).